

# INFLUENCES OF THE NEAR-WALL DRAG CORRECTION IN A LAGRANGIAN SIMULATION OF PARTICULATE TURBULENT CHANNEL FLOW

Koji Fukagata<sup>1,3</sup>, Said Zahrai<sup>2,3</sup>, Fritz H. Bark<sup>3</sup> and Shunsuke Kondo<sup>1</sup>

<sup>1</sup> Department of Quantum Engineering and Systems Science, The University of Tokyo  
7-3-1 Hongo, Bunkyo-ku, Tokyo 113-8656, Japan

<sup>2</sup> ABB Corporate Research  
721 78 Västerås, Sweden

<sup>3</sup> FaxénLaboratoriet, Kungl. Tekniska Högskolan  
100 44 Stockholm, Sweden

## ABSTRACT

A gas-particle turbulent channel flow is simulated using a large eddy simulation coupled with Lagrangian particle tracking. A turbulent channel flow at  $Re_\tau = 644$ , loaded with  $70\text{ }\mu\text{m}$  copper particles at a mass fraction of 2%, is considered and influences of the increase of drag coefficient near the wall on the statistics of particles are investigated. Three different types of coupling mechanisms, two different drag coefficients and two different boundary conditions are examined. The accumulated statistics are compared with the experimental data by Kulick et al. (1994). The statistics computed by the simulation with both wall correction and inter-particle collisions are found to be closer to the experimental data, as compared to statistics from typical conventional simulations which neglect those effects.

## INTRODUCTION

Gas-particle turbulent channel flows have been studied by many researchers theoretically, experimentally and numerically. Among different methods in numerical simulations, it is considered in principle that the Lagrangian particle tracking coupled with a direct numerical simulation (DNS) or a large eddy simulation (LES) is able to predict such flows with high accuracy. But, unfortunately, previous researches using DNS or LES with particle tracking, e.g. Wang and Squires (1996) who performed one-way coupling simulation, could not reproduce the experimental data by Kulick et al. (1994) with a reasonable accuracy.

Recently, Tanaka et al. (1997) showed that the inter-particle collisions have a strong influence on the statistics of particle velocity even at low mass flow ratio,  $Z$ , of 20%. In particular, they demonstrated that the transverse RMS particle velocity fluctuations were almost twice as large in a

simulation with inter-particle collisions as those in the simulation without collisions. However, in the case with much smaller particle mass flow ratio, such as  $Z = 2\%$  dealt with in the experiment by Kulick et al., the large deviation from experimental data may not be explained only by the neglect of inter-particle collisions because the influence of inter-particle collisions may be twice less important as compared with that in the case of  $Z = 20\%$ . Also, in the experiment at  $Z = 2\%$  by Kulick et al., a strange bimodal behavior was observed in the probability density function of particle velocity near the wall. Such bimodality has not clearly been observed in the previous simulations. Therefore still other reasons for disagreement between prediction and experimental data should be explored for this case.

As Faxén (1923) derived analytically using the method of reflections, the drag coefficient in the direction parallel to the wall increases when a particle is located near a plane wall. The drag coefficient in the direction normal to the wall is also known to increase near the wall, as solved by Brenner (1961) using bipolar coordinates.

Rizk and Elghobashi (1984) took into account the effect of walls on particle drag in a  $k\text{-}\epsilon$  based two-fluid model simulation of a turbulent channel flow of air loaded with polystyrene particles and compared the results with the experimental data by Tsuji et al. (1984). Pan and Banerjee (1996) implicitly included this effect through their two-way coupling model, i.e. velocity model, in a DNS with Lagrangian particle tracking of liquid-particle flows and compared the results with the experimental data by Rashidi et al. (1990). They both obtained quite good agreement as compared to the corresponding experimental data.

However, this effect has often been neglected in the Lagrangian particle tracking simulations of gas-particle turbulent channel flows. One of the difficulties in incorporating

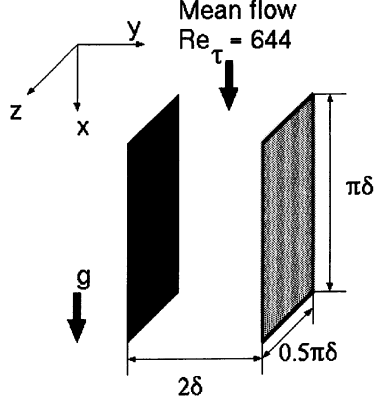


Figure 1: Geometry of the channel.

this effect is that there is no relevant expression for it when the particle Reynolds number is higher than the Stokes limit. Such situation does not occur in the liquid-particle system treated in the simulation by Pan and Banerjee where the particle Reynolds number was considered to be very low.

The objective of the present study is to examine the influences of the drag correction factor for the Stokes flow on the particle statistics in a Lagrangian particle tracking simulation of very dilute gas-particle turbulent channel flow. Comparisons are made with the experimental data by Kulick et al. (1994) who studied the statistics of 70  $\mu\text{m}$  copper particles at  $Z = 2\%$  loading in a turbulent channel flow at  $Re_\tau = 644$ .

## METHODOLOGY

Since the near-wall behavior of particles is studied, DNS may be considered a better simulation technique. However, the feasibility of DNS is still restricted to low Reynolds numbers, e.g.  $Re_\tau = 162$  in a recent DNS by Lamballais (1996). In order to study the motion of 70  $\mu\text{m}$  copper particles near the wall, one should compute the particle motion with a reasonable accuracy not only near the wall but also in entire channel. That is due to the fact that the relaxation time of particle is large,  $\tau_p^+ = 2000$ , resulting in a direct coupling between near-wall characteristics of particle statistics and that in the center of the channel. Therefore in this study, an LES with a modified Smagorinsky subgrid scale model (Zahrai et al., 1995) was adopted to simulate the turbulent channel flow at  $Re_\tau = 644$ .

The channel has a half width,  $\delta$ , of 2 cm in  $y$  direction and infinitely large dimensions in the streamwise,  $x$ , and the spanwise,  $z$ , directions in the physical space. The dimensions of the computational domain is  $\pi\delta \times 2\delta \times 0.5\pi\delta$  in  $x$ ,  $y$  and  $z$  directions, as shown in Figure 1, with periodic boundary conditions applied in  $x$  and  $z$  directions.

The wall corrections on drag, introduced in the following, rest on the assumption of small, or possibly moderately small, values of the particle Reynolds number,  $Re_p$ , defined by

$$Re_p = |\vec{u}^{+p} - \vec{u}^{+f}| d^+ \quad (1)$$

where  $\vec{u}^{+p}$  and  $\vec{u}^{+f}$  are the velocities of the particle and the fluid at particle center, respectively, and  $d^+$  is the diameter of

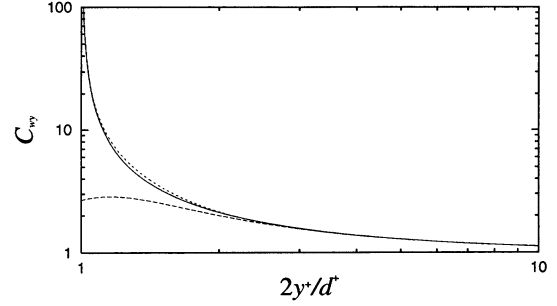


Figure 2: Drag correction normal to the wall.

—, exact solution by Brenner (1961);  
 — —, approximate solution by Wakiya (1960);  
 - - - -, model in this study.

the particles. The superscript, +, denotes the variables in wall unit.

The motion of particles was computed individually by integrating the particle equation of motion,

$$\frac{du_i^{+p}}{dt^+} = C_{Re_p} C_{wi} \frac{1}{\tau_p^+} (u_i^{+f} - u_i^{+p}) + g_i^+ \quad (2)$$

where  $\tau_p^+$  is the Stokes relaxation time.  $g_i^+$  is the gravity. The first correction factor,  $C_{Re_p}$ , is the correction for higher particle Reynolds number than the Stokes limit (Schiller and Naumann, 1933),

$$C_{Re_p} = 1 + 0.15 Re_p^{0.687} \quad (3)$$

The second correction factor,  $C_{wi}$ , where the subscript  $i$  reads  $x$ ,  $y$  or  $z$ , is the correction near the wall. For the direction parallel to the wall, the expression by Faxén (1923),

$$C_{wx} = C_{wz} = \left[ 1 - \frac{9}{16} \left( \frac{d^+}{2y^+} \right) + \frac{1}{8} \left( \frac{d^+}{2y^+} \right)^3 - \frac{45}{256} \left( \frac{d^+}{2y^+} \right)^4 - \frac{1}{16} \left( \frac{d^+}{2y^+} \right)^5 \right]^{-1} \quad (4)$$

was used.

For the direction normal to the wall, several expressions have been proposed. One of them is the approximate solution by Wakiya (1960),

$$C_{wy} = 1 - \frac{9}{8} \left( \frac{d^+}{2y^+} \right) + \frac{1}{2} \left( \frac{d^+}{2y^+} \right)^2 \quad (5)$$

Although this is as simple as the expression for  $C_{wx}$  by Faxén, it underestimates the correction factor in the vicinity of the wall, say  $2y^+/d^+ < 2$ , as shown in Figure 2. The exact solution by Brenner (1961) can be written as

$$C_{wy} = \frac{4}{3} \sinh \alpha \sum_{n=1}^{\infty} \frac{n(n+1)}{(2n-1)(2n+3)} \cdot \left[ \frac{2 \sinh(2n+1)\alpha + (2n+1) \sinh 2\alpha}{4 \sinh^2(n+\frac{1}{2})\alpha - (2n+1)^2 \sinh^2 \alpha} - 1 \right] \quad (6)$$

where  $\alpha$  is defined by  $\alpha = \cosh^{-1}(2y^+/d^+)$ . It shows an exponential behavior when  $2y^+/d^+$  approaches to unity. In the present study, a model formula, which is a combination of the simple expression by Wakiya and the exponential behavior in the solution of Brenner,

$$C_{wy} = \left[ \left\{ 1 - \frac{9}{8} \left( \frac{d^+}{2y^+} \right) + \frac{1}{2} \left( \frac{d^+}{2y^+} \right)^2 \right\} \cdot \left\{ 1 - \exp \left( -a \left( \frac{2y^+}{d^+} - b \right) \right) \right\} \right]^{-1} \quad (7)$$

was used to save computing time, rather than computing formula (6) directly.

Although the constant,  $b$ , is 1 in order to obtain the similar exponential behavior as the exact solution,  $b = 0.9999$  was used in the simulations to avoid calculations of infinite numbers. The constant  $a$  was determined by a least-square fit using 2000 points between  $2y^+/d^+ = 1$  and  $2y^+/d^+ = 3$  from the exact solution, resulting in  $a = 2.686$ .

One-way, two-way and four-way coupling simulations, whose meanings are explained in table 1, were performed. Two-way coupling was computed by a force coupling method, similarly as the previous work by the authors (Fukagata et al., 1998a). In four-way coupling, perfectly elastic collisions were assumed between two colliding particles and the momentum change of these particles were computed directly using the momentum conservation law. To determine the colliding pair, the same method as Yamamoto et al. (1998) was used.

In all cases, copper particles with a diameter of  $70\mu\text{m}$ , which corresponds to  $d^+ = 2.3$ , were considered. The Stokes relaxation time,  $\tau_p^+$ , was 2000. Totally 250000 particles were tracked in one-way coupling simulations, and 1600 particles in two-way and four-way coupling simulations. The number of particles used in the two-way and four-way coupling simulations in the present study corresponds to mass concentration,  $C$ , of 2% and the volume fraction at  $3.7 \times 10^{-6}$ .

Following the definitions in the monograph by Crowe et al. (1998), the mass loading,  $Z$ , is defined as the ratio of particle flux to fluid flux, while the mass concentration,  $C$ , is defined as the ratio of total mass of particles to fluid mass. Obviously, these two quantities differ when the particle velocity and the fluid velocity differ. In order to realize  $Z = 2\%$  in the simulation, the number of particles should be controlled using the statistics being computed. However, in this study  $C = 2\%$ , i.e. fixed number of particles, was used for simplicity in computations. It is difficult to estimate in advance the error introduced by using  $C = 2\%$  instead of  $Z = 2\%$ . In all the cases examined in this study, the value of  $Z$  were between 1.5% and 2.2%, which were computed after the simulations.

The simulations were performed as the following. At

Table 1: One-way, two-way and four-way couplings.

	Influence of fluid motion on particle motion	Influence of particle motion on fluid motion	Collisions between particles
One-way	yes	no	no
Two-way	yes	yes	no
Four-way	yes	yes	yes

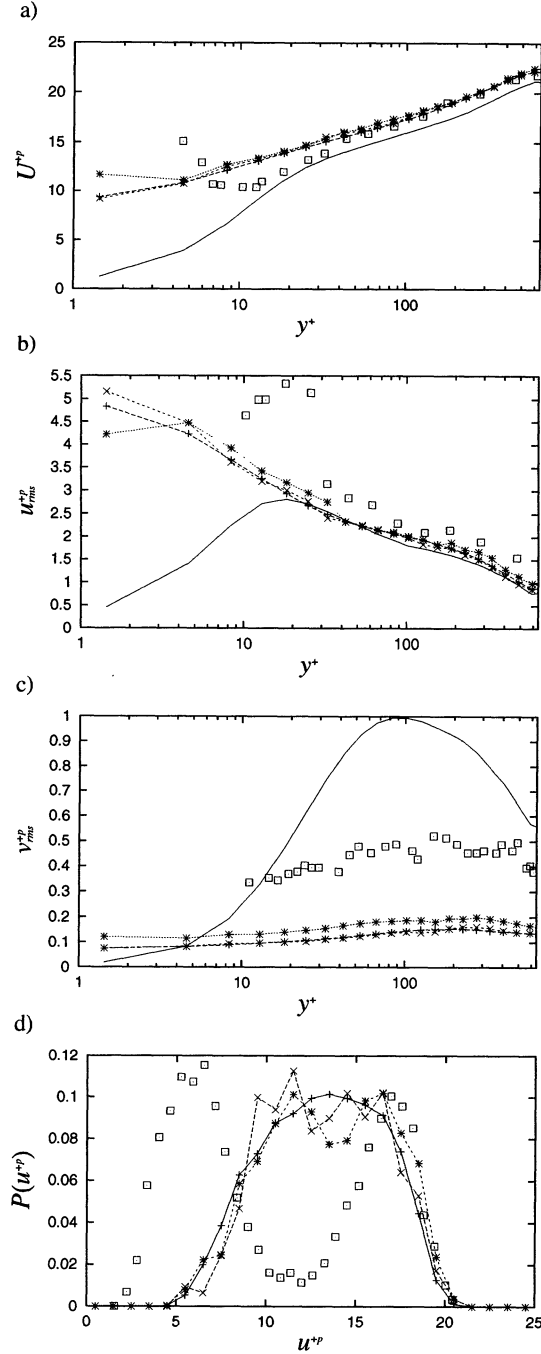


Figure 3: Statistics of particles from simulations with different couplings. a) mean velocity; b) RMS streamwise velocity; c) RMS wall normal velocity; d) PDF of streamwise particle velocity at  $y^+ = 12$  plane.

— + —, Case 1a, i.e. one-way;  
 - - × - -, Case 2a, i.e. two-way;  
 ··· \* ···, Case 4a, i.e. four-way;  
 □, experiment by Kulick et al. (1994),  $Z = 2\%$ ;  
 (——), undisturbed fluid. )

Table 2: Studied cases.

One-way coupling	Case 1a	Case 1b	-
Two-way coupling	Case 2a	-	-
Four-way coupling	Case 4a	Case 4b	Case 4c
Drag correction	no	yes	yes
Bounce at the wall	yes	yes	no

$t^+ = 0$ , particles were homogeneously distributed in whole channel. The initial particle velocities were set to the local fluid velocities. The statistics were accumulated for about 4000 wall unit times after the flows were considered to have reached convergence by monitoring the momentum balance of particles (Fukagata et al., 1998b).

## RESULTS

### Effects of different coupling mechanisms

First of all, the simulations were carried out with three different couplings, i.e. one-way in *Case 1a*, two-way in *Case 2a* and four-way in *Case 4a*, as shown in table 2. The drag correction factor near the wall was not taken into account in these cases. The particles were assumed to bounce elastically at the walls.

Figure 3a and 3b show that in *Case 4a* the mean particle velocity,  $U^{+p}$ , is higher and the root-mean-square (RMS) level of streamwise particle velocity,  $u_{rms}^{+p}$ , is lower very near the wall, as compared to the those in *Case 1a* and *Case 2a*.

The RMS level of wall-normal particle velocity,  $v_{rms}^{+p}$ , as shown in Figure 3c, is higher in the whole channel in *Case 4a* than in *Case 1a* and *Case 2a*. Although the values of  $v_{rms}^{+p}$  are still lower than the experimental data by Kulick et al. (1994), this result may suggest that the particle collisions should not be neglected even at a mass fraction as low as 2%.

The probability distribution function (PDF) of streamwise particle velocity at  $y^+ = 12$  plane,  $P(u^+)$ , as shown in Figure 3d shows that the PDFs in *Case 1a* and *Case 2a* seem to consist of only one mode and that in *Case 4a* seems to be bimodal. However, the mean value of the lower mode in *Case 4a*, provided that it is bimodal, is much higher than that in the experimental data.

### Effects of near-wall drag

Simulations were continued to investigate the influences of near-wall drag correction factor, formulas (4) and (7), on the statistics of particles. Since the results in the previous section have shown that the inter-particle collisions cannot be neglected, a four-way coupling simulation with drag correction, referred to as *Case 4b*, was carried out and comparison was made with the data from the four-way coupling simulation without drag correction, *Case 4a*. In order to see whether the particle statistics become closer to experimental data only by including near-wall drag correction, a one-way coupling simulation with drag correction, *Case 1b*, was also performed. As in the previous section, the particles were assumed to bounce elastically at the walls.

The mean velocities are shown in Figure 4a. The values of  $U^{+p}$  at the point closest to the wall are lower in the cases with near-wall drag correction, i.e. *Case 4b* and

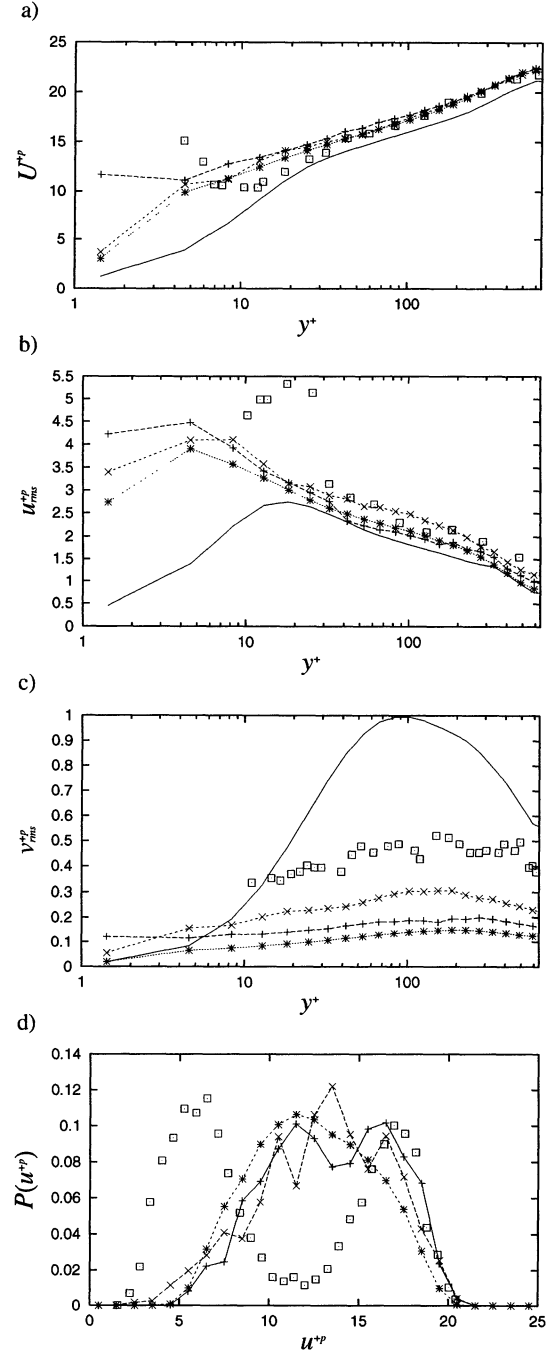


Figure 4: Particle statistics with or without near-wall drag correction. a) mean velocity; b) RMS streamwise velocity; c) RMS wall normal velocity; d) PDF of streamwise particle velocity at  $y^+ = 12$  plane.

— + —, *Case 4a*, i.e. four-way without drag correction;  
 - - x - -, *Case 4b*, i.e. four-way with drag correction;  
 ··· \* ···, *Case 1b*, i.e. one-way with drag correction;  
 □, experiment by Kulick et al. (1994),  $Z = 2\%$ ;  
 (—, undisturbed fluid.)

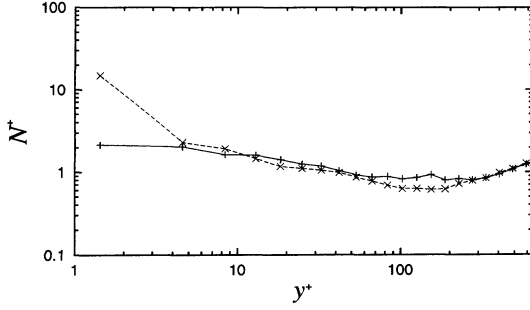


Figure 5: Particle number density profile.  
 - + -, Case 4a, i.e. without drag correction;  
 - x -, Case 4b, i.e. with drag correction.

Case 1b, than in Case 4a. The main reason may be that the particles near the wall slow down due to large streamwise drag. An other possible reason may be that the particles stay longer in the near-wall region due to large wall-normal drag and the streamwise particle velocities are relaxed more to the slow velocity of the fluid.

The RMS values of streamwise velocity are shown in Figure 4b. Again, Case 4b and Case 1b gave lower  $u_{rms}^{+p}$  near the wall due to the same reason as that for  $U^{+p}$ .

Figure 4c shows the RMS wall-normal velocities. The values of  $v_{rms}^{+p}$  in Case 4b are much higher in the whole channel than those in Case 4a. On the other hand,  $v_{rms}^{+p}$  in Case 1b were lower than those in Case 4a.

The PDFs of streamwise particle velocity at  $y^+ = 12$  plane are shown in Figure 4d. Clear bimodal behavior cannot be seen in Case 4b and the shape of the PDF computed here is zigzag-like. Whether such shape is due to the limited number of sample data or not will be studied later.

In Case 4b, particles tend to accumulate more in the near-wall region, as shown in Figure 5. The frequency of inter-particle collisions are considered to increase as the number density increases. As a result,  $v_{rms}^{+p}$  is also likely to increase because some parts of streamwise particle velocities is converted to transverse velocities through the collision process. Therefore the larger  $v_{rms}^{+p}$  in the near-wall region in Case 4b compared to that in Case 4a may be due to a larger collision frequency accompanied by the higher particle number density near the wall. The large  $v_{rms}^{+p}$  found in the bulk region, where particle collisions are not frequent, may be explained by the large particle relaxation time,  $\tau_p^+ = 2000$ .

### Effects of momentum loss at walls

In the following simulations, the particles hitting the wall are assumed to lose their momentum, i.e.  $\vec{u}^{+p} = \vec{0}$ , such that more particles are tend to accumulate in the near-wall region. After the momentum a particle was lost at the wall, the particle was treated to be accelerated again by the drag force and leave the wall region. This case of four-way coupling simulation with drag correction and no-bounce, no-slip boundary condition is referred as Case 4c.

Figure 6a shows that  $U^{+p}$  is lower in Case 4c,

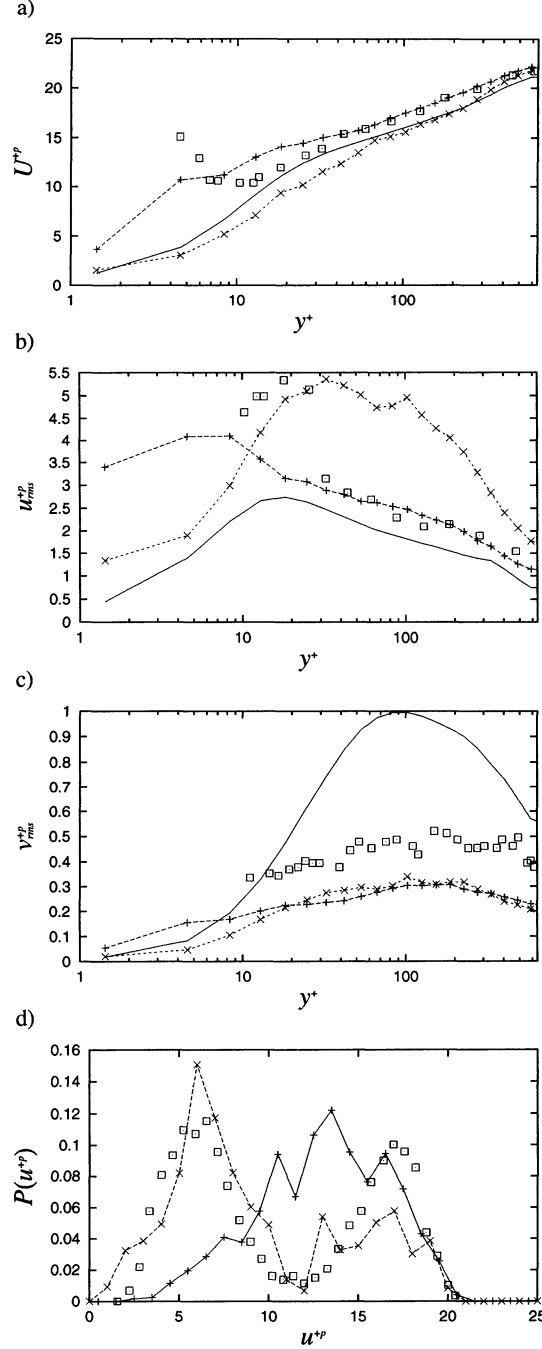


Figure 6: Particle statistics with different boundary conditions. a) mean velocity; b) RMS streamwise velocity; c) RMS wall normal velocity; d) PDF of streamwise particle velocity at  $y^+ = 12$  plane.

- + -, Case 4b, i.e. elastic bounce;  
 - x -, Case 4c, i.e. no-bounce, no-slip;  
 □, experiment by Kulick et al. (1994),  $Z = 2\%$ ;  
 (—), undisturbed fluid. )

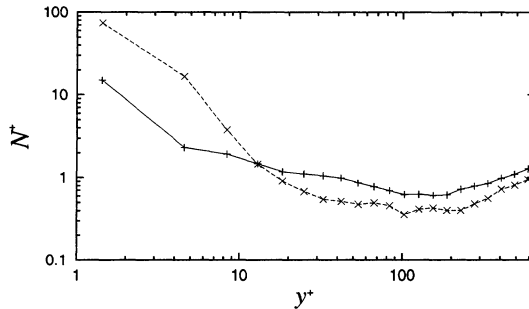


Figure 7: Particle number density profile.  
 - + -, Case 4b, i.e. elastic bounce;  
 - - x -, Case 4c, i.e. no-bounce, no-slip.

especially in the viscous sublayer, than those in Case 4b and the experimental data.

Figure 6b shows the profile of  $u_{rms}^{+p}$ . In the buffer layer, the values in Case 4c are quite similar to the experimental data. However, in the logarithmic layer,  $u_{rms}^{+p}$  in the experiment is similar to that in Case 4b rather than Case 4c.

In Figure 7, the particle number density near the wall in Case 4c is higher than that in Case 4b. However, the values of  $v_{rms}^{+p}$  in Case 4c stay at the comparable level as those in Case 4b, as shown in Figure 6c. The  $v_{rms}^{+p}$  is lower than expected may be due to the lower mean and RMS values of  $u^{+p}$ , which results in lower values of  $v^{+p}$  through the collision process.

The PDF in Case 4c, as shown in Figure 6d, has a different character compared to Case 4b. The bimodality can clearly be seen with the mean value and magnitude for each mode comparable to the experimental data. In the experiment more particles may stay near the wall as compared to Case 4c. This difference may be the cause of the smaller probability of the lower mode and a higher  $U^{+p}$ .

## CONCLUSIONS

Computations of 70  $\mu\text{m}$  copper particles in a turbulent channel flow were performed using large eddy simulation coupled with Lagrangian particle tracking in order to simulate the experiment by Kulick (1994) at mass ratio of 2%.

The simulations with different coupling showed that the inter-particle collisions should not be neglected even at a low mass fraction,  $C = 2\%$ .

The four-way coupling simulations with or without drag correction near the wall showed that the near-wall drag correction has a strong influence on the particle statistics, especially on the wall-normal velocity fluctuations of particles. However, the agreement with the experimental data was still not satisfactory.

Different boundary conditions were considered in the four-way coupling simulation with near-wall drag correction. The statistics from the simulation with no-bounce, no-slip boundary conditions are fairly close to experimental data in the buffer layer but not in the logarithmic region. This indicates that the particle behavior at the wall in the experiment might be closer to no-bounce rather than elastic bounce.

## REFERENCES

- Brenner, H., 1961, "The Slow Motion of a Sphere through a Viscous Fluid towards a Plane Surface," *Chemical Engineering Science*, Vol. 16, pp. 242-251.
- Crowe, C., Sommerfeld, M. and Tsuji, Y., 1998, "Multiphase Flows with Droplets and Particles," CRC Press.
- Faxén, H., 1923, "Die Bewegung einer starren Kugel Längs der Achse eines mit zäher Flüssigkeit gefüllten Rohres," *Arkiv för Matematik, Astronomi och Fysik*, Vol. 17, No.27, pp. 1-28.
- Fukagata, K., Zahrai, S. and Bark, F. H., 1998a, "Fluid Stress Balance in a Turbulent Particulate Channel Flow," *Proceedings of 3rd International Conference on Multiphase Flow (CD-ROM)*, Paper 157, pp. 1-8.
- Fukagata, K., Zahrai, S. and Bark, F. H., 1998b, "Force Balance in a Turbulent Particulate Channel Flow," *International Journal of Multiphase Flow*, Vol. 24, pp. 867-887.
- Kulick, J. D., Fessler, J. R. and Eaton, J. K., 1994, "Particle Response and Turbulence Modification in Fully Developed Channel Flow," *Journal of Fluid Mechanics*, Vol. 277, pp. 109-134.
- Lamballais, E., 1996, "Simulations numériques de la turbulence dans un canal plan tournant," Thèse de l'Institut National Polytechnique de Grenoble.
- Pan, Y. and Banerjee, S., 1996, "Numerical Simulation of Particle Interactions with Wall Turbulence," *Physics of Fluids*, Vol. 8, pp. 2733-2755.
- Rashidi, M., Hetsroni, G. and Banerjee, S., 1990, "Particle-turbulence interaction in a boundary layer," *International Journal of Multiphase Flow*, Vol. 16, pp. 935-949.
- Rizk, M. A. and Elghobashi, S. E., 1989, "A Two-Equation Turbulence Model for Dispersed Dilute Confined Two-Phase Flows," *International Journal of Multiphase Flow*, vol. 15, pp. 119-133.
- Schiller, L. and Naumann, A., 1933, "Über die grundlegenden Berechnungen bei der Schwerkraftaufbereitung," *Vereines Deutscher Ingenieure*, vol. 77. p. 318.
- Tanaka, T., Yamamoto, Y., Potthoff, M. and Tsuji, Y., 1997, "LES of Gas-Particle Turbulent Channel Flow," *Proceedings of 1997 ASME Fluid Engineering Division Summer Meeting (CD-ROM)*, FEDSM97-3630, pp. 1-5.
- Tsuji, Y., Morikawa, Y. and Shiomi, H., 1984, "LDV measurement of an air-solid two-phase flow in a vertical pipe," *Journal of Fluid Mechanics*, Vol. 139, pp. 417-434.
- Wakiya, S. J., 1960, *Research Report 9*, Faculty of Engineering, Niigata Univ., Japan.
- Wang, Q. and Squires, K. D., 1996, "Large Eddy Simulation of Particle-Laden Turbulent Channel Flow," *Physics of Fluids*, Vol. 8, pp. 1207-1223.
- Yamamoto, Y., Tanaka, T. and Tsuji, Y., 1998, "LES of Gas-Particle Turbulent Channel Flow (The Effect of Inter-Particle Collision on Structure of Particle Distribution)," *Proceedings of 3rd International Conference on Multiphase Flow (CD-ROM)*, Paper 518, pp. 1-7.
- Zahrai, S., Bark, F. H. and Karlsson, R. I., 1995, "On Anisotropic Subgrid Modeling," *European Journal of Mechanics, B/Fluids*, Vol. 14, pp. 459-486.